Atmospheric Environment 309 (2023) 119952

Contents lists available at ScienceDirect

Atmospheric Environment

journal homepage: www.elsevier.com/locate/atmosenv

Effects of boundary layer dynamics and meteorology on ultrafine particle formation and growth

Zachary Watson [a], Lee Tiszenkel [b], Arastoo Pour Biazar [c], Kevin Knupp [b,c], Shan-Hu Lee [b,c,*]

[a] Department of Meteorology, Florida Institute of Technology, Melbourne, FL, USA
[b] Department of Atmospheric and Earth Sciences, University of Alabama in Huntsville, Huntsville, AL, USA
[c] Earth System Science Center, University of Alabama in Huntsville, Huntsville, AL, USA

HIGHLIGHTS

- Historically, meteorology and atmospheric chemistry fields have been "segregated" and often, they don't work together.
- Thus, the link between meteorology and aerosol formation was not extensively studied experimentally.
- We show long-term co-located measurements of aerosol size distributions and Lidar in the southeastern United States.
- Our observations show clear effects of meteorology on aerosol formation and growth.

ARTICLE INFO

Keywords:
Ultrafine particles
New particle formation
Atmospheric dynamics
Boundary layer
Meteorology

ABSTRACT

It is currently not well understood how the planetary boundary layer (PBL) dynamics affects the formation and growth of ultrafine particles in the atmosphere, because of the limited co-located aerosol size distributions and lidar measurements. Here we show, from long-term in-situ observations, a clear link between boundary layer processes and surface aerosol dynamics. Aerosol size distributions in the diameter range from 7 to 300 nm were measured with a scanning mobility particle sizer (SMPS) at the University of Alabama Huntsville campus in 2016, 2017, and 2022. The backscatter of larger aerosols was measured using a co-located lidar ceilometer. Meteorological surface parameters including temperature, relative humidity, station pressure, wind speed and direction, solar radiation, and precipitation were also measured. New particle formation (NPF) and long growth (over 12 h) events occurred most frequently during the winter, unlike many other locations where NPF events occur more frequently in spring and fall, indicating that cooler temperatures play important roles in ultrafine particle formation in the warm subtropical environment. During the summer with strong solar radiation, there were more short-time growth events (less than 6 h), likely associated with convection within the boundary layer. Our observations also show cold fronts affect the measured aerosol size distributions because the combination of precipitation scavenging and cleaner air can provide thermodynamic conditions favorable for NPF and aerosol growth. These results highlight the importance of meteorology on aerosol formation and growth.

1. Introduction

New particle formation (NPF) is the main source of ultrafine particles (UFP) in the atmosphere and contributes significantly to the global cloud condensation nuclei (CCN) production. Recent studies have shown that various chemical precursors, such as sulfuric acid, ammonia, amines, highly oxygenated organic molecules (HOMs), and iodide oxides can contribute to the formation and growth of new particles (Lee et al., 2019; Kerminen et al., 2018). Atmospheric dynamical processes such as storms, boundary layer processes, turbulence, and atmospheric waves can enhance NPF (Nilsson et al., 2001; Nyeki et al., 1999; Kulmala et al., 1998; Wehner et al., 2010; Boulon et al., 2011; Siebert et al., 2004; Lai et al., 2022; Wu et al., 2021). This is because these processes may produce high supersaturation ratios of water vapor in the atmosphere by rapidly mixing air masses with high humidity and low temperatures. Because nucleation is a non-linear process, even minor fluctuations in temperature and relative humidity (RH) can increase nucleation rates over several orders of magnitude. Convection can also transport higher

* Corresponding authorDepartment of Atmospheric and Earth Sciences, University of Alabama in Huntsville, Huntsville, AL, USA
E-mail address: shanhu.lee@uah.edu (S.-H. Lee).

https://doi.org/10.1016/j.atmosenv.2023.119952
Received 19 April 2023; Received in revised form 7 July 2023; Accepted 8 July 2023
Available online 13 July 2023

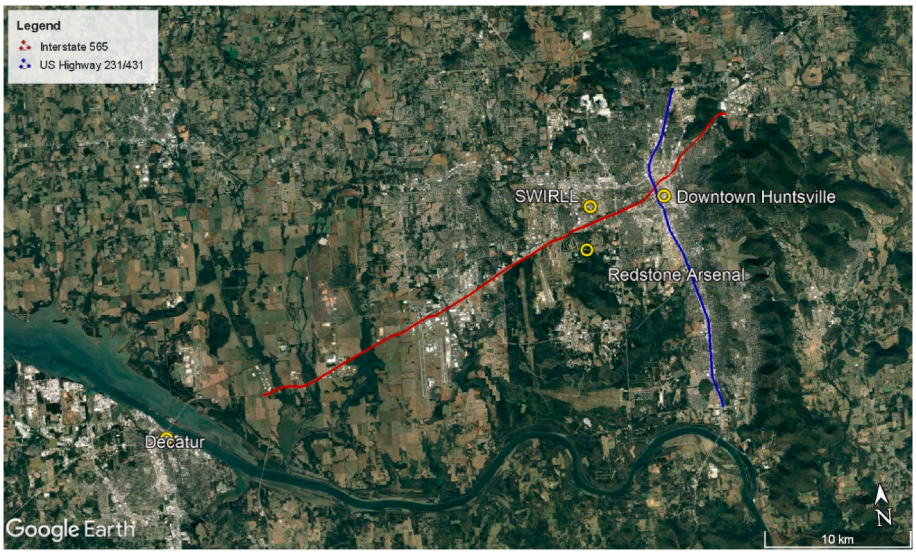

Fig. 1. A Google Earth satellite imagery of the Huntsville area with labels showing the location of the measurement site at SWIRLL and probable sources of anthropogenic UFP. These sources include the highly traveled freeways of Interstate 565 (red line) and US Highway 231/431 (blue line), and locations such as Decatur, Alabama, Redstone Arsenal, and Downtown Huntsville, Alabama.

concentrations of nucleation precursors produced from the ground level into the free troposphere (Kalivitis et al., 2015; Rönkkö et al., 2017; Guo et al., 2020; Stull et al., 1998; Alabama Department of Transportation; Yu et al., 2014). Thus, the combination of colder temperatures, higher humidity, the lower surface area of preexisting aerosol particles, and higher precursor concentrations associated with convection can create an ideal condition for NPF in the free troposphere (Alabama Department of Transportation; Yu et al., 2014; Zhang et al., 2022).

It is possible that new particles formed in the free troposphere can also be transported via downdrafts to the surface (Wehner et al., 2010; Wang et al., 2016, 2023; Fan et al., 2018; Lampilahti et al., 2021; Liu et al., 2021). For example, this downdraft process can serve as a main source of UFP in the Amazon rainforest where the local NPF does not occur, by "recycling" new particles formed in the cool free troposphere induced by biogenic nucleation precursors uplifted from the ground level (Wang et al., 2016; Fan et al., 2018; Williamson et al., 2019). Lai et al. (2022) showed that vertical mixing within the boundary layer can also enhance NPF at the surface in polluted Northern China. Chen et al. (2018) observed that ultrafine particles that were generated at the top region of the boundary layer are rapidly mixed throughout the boundary layer at the Southern Great Plains site in Oklahoma. Meskhidze et al. (2019) suggested that large concentrations of particles freshly produced above the boundary layer can be brought to the surface by boundary layer growth and daytime mixing to become an important source of aerosol particles at the ground level at an urban site in North Carolina.

However, there are still very limited NPF studies that have detailed profiles of atmospheric boundary layer dynamics from in-situ observations; for example, most of the previous studies use the model-simulated boundary layer heights. Also, long-term measurements of simultaneous measurements of NPF and boundary layer dynamics are scarce. Here, we show long-term observations of aerosol size distributions, lidar ceilometer, and the ambient meteorological conditions in Huntsville, Alabama over four seasons to understand the link between the boundary layer dynamics and the surface UPF in the southeastern United States (US).

2. Methods

The measurement were made at the Severe Weather Institute and Radar & Lightning Laboratories (SWIRLL) building (https://www.nsstc.uah.edu/swirll/main/platforms/sfc.php) (34°43′29″ N, 86°38′47″ W, 212 m above mean sea level) at the University of Alabama in Huntsville (UAH) in Huntsville, Alabama. The aerosol sampling was taken from the roof of the SWIRLL building with the inlet 10 m above the ground. The lidar ceilometer and meteorology measurements were made at the surface.

Fig. 1 shows the UAH and the surrounding Huntsville area. Huntsville has a population of 217,000 and is the largest city in the state of Alabama. The UAH campus is located approximately 10 km west of downtown Huntsville, 1 km north of Interstate Highway 565 and 4.5 km to the east of US Highway 231/431. The main industry in the region takes place in Decatur, located approximately 30 km to the southwest of UAH. There are also military exercises at Redstone Arsenal, about 10 km to the south of UAH.

Aerosol size distributions in the diameter range of 7–300 nm were measured with a scanning mobility particle sizer (SMPS). The SMPS has two components: a differential mobility analyzer (DMA, TSI 3081) and a butanol-based condensation particle counter (CPC, TSI 3772). In this study, particles within the size range fro 7–300 nm were loosely defined as UFP. The UFP events were classified into two main categories: (1) UFP from NPF with characteristic "banana" shaped aerosol size distributions, and (2) UFP associated with sustained aerosol growth (typically longer than 12 h), as discussed in the following section.

Growth rates (GR) were calculated based on the measured aerosol size distribution:

$$GR = \frac{dD_p}{dt} \approx \frac{D_f - D_i}{dt} \tag{1}$$

where dD_p is the change in median diameter from the beginning to the end of the growth event, D_i is the initial particle size, D_f is the final particle size, and dt is the length of the growth event. The standard deviations for GR (σ_{GR}) were determined using propagated error techniques. The standard deviation for the initial (σ_{Di}) and final (σ_{Df}) particle sizes were calculated from the aerosol size distribution, and the accuracy of the estimation of event length was 15 min (σ_{dt}). The propagated error formula for GR based on Equation (1) is:

$$\sigma_{GR} = \sqrt{\frac{(dt)^2\left(\sigma_{Df}{}^2 + \sigma_{Di}{}^2\right) + \sigma_{dt}{}^2\left(D_f - D_i\right)^2}{(dt)^4}} \tag{2}$$

where σ_{Di} and σ_{Df} are the standard deviations of the initial and final particle diameters.

A Vaisala CL51 lidar ceilometer was used to obtain aerosol

Table 1
Summary of the measured aerosol and meteorology data averaged during different seasons. Numbers in parentheses correspond to the number of days of data available to calculate that particular average. Aerosol quantities are expressed with an error of one standard deviation (±1σ). The overall mean values were calculated using a weighted average for each season, and the overall standard deviations were weighted by degrees of freedom of the seasonal standard deviations (sample size – 1).

Parameter	Winter (DJF)	Spring (MAM)	Summer (JJA)	Autumn (SON)	Overall
7–300 nm UFP Concentration (cm^{-3})	(5.3 ± 3.3) × 10^3 (58)	(4.9 ± 3.0) × 10^3 (47)	(4.5 ± 2.4) × 10^3 (44)	(4.4 ± 2.1) × 10^3 (50)	(4.8 ± 2.8) × 10^3 (199)
NPF Frequency (% of days)	24 (58)	26 (47)	11 (44)	12 (50)	19 (199)
Growth Rate (nm hr^{-1})	2.2 ± 4.8 (12)	1.8 ± 5.0 (10)	1.2 ± 4.9 (1)	2.7 ± 3.9 (6)	1.7 ± 4.7 (29)
Daily Maximum PBL Height (m)	1450 ± 500 (27)	1550 ± 450 (32)	1800 ± 350 (34)	1900 ± 300 (35)	1700 ± 450 (128)
2 m Air Temperature (°C)	8.0 ± 5.9 (57)	14.5 ± 4.8 (47)	27.7 ± 1.7 (35)	23.5 ± 4.1 (50)	17.4 ± 8.9 (189)

backscatter profiles. The lidar has a wavelength of 910 nm and has a vertical range from 0 to 15 km, detecting up to three cloud bases. The purpose of using backscatter profiles obtained from the ceilometer was to identify the planetary boundary layer (PBL) height, as well as the presence of clouds and rain fall events. This study will focus on 0–4 km backscatter profiles.

The surface meteorological were measured with a suite of instruments: Campbell Scientific 107 temperature probe for 2-m air temperature, Vaisala HMP-45C temperature/relative humidity probe for 2-m relative humidity, Vaisala PTB-210 barometer for station pressure, RM Young 05103 Wind Monitor for 10-m wind speed and direction, Texas Instruments TR-525I rain gauge to track rainfall, and an Eppley Labs Pyranometer for solar radiation measurements.

Table S1 summarizes the measurement data of the SMPS, lidar ceilometer, and the surface meteorology parameters. The SMPS was active from 30 June 2016 to 14 April 2017, and from 1 January 2022 to 23 March 2022. In total, 199 days of data of SMPS measurements, crossing four seasons, are included in this study.

3. Results and discussion

3.1. Overview and seasonality

For the seasonality analysis, we defined the seasons as the following: spring from March to May (MAM), summer from June to August (JJA), autumn form September to November (SON), and winter from December to February (DJF). Table 1 summarizes the seasonally averaged measurements of UFP concentrations in the diameter from 7 to 300 nm, NPF frequencies, overall GR, PBL heights, and 2 m air temperature.

NPF events were most common in the spring (26%), then the winter (24%), autumn (12%), and least common in the summer (11%) (Table 1). Our results agree with previous studies that suggest NPF events are the most common in the spring, but disagree that NPF is the least common in the winter in many other locations (Lee et al., 2019; Kerminen et al., 2018). For example, from 4 years of long-term observations of NPF in Kent, Ohio, Kanawade et al. (2012) showed that NPF was most common in the spring, then autumn, summer, with the least NPF events in winter. Our results suggest that low temperatures are especially important for NPF in the relatively warm climate in the sub-tropics. Colder temperatures are more favorable for UFP formation (Wang et al., 2016), as high temperatures can cause evaporation of freshly nucleated particles (Lee et al., 2019).

Particle number concentrations also showed the similar seasonality, highest in the wintertime at (5.3 ± 3.3) × 10^3 cm^{-3} and lowest in the autumn at (4.4 ± 2.1) × 10^3 cm^{-3}. The number concentrations for all seasons can be seen in Table 1. This was likely due to the lower PBL heights seen during the colder weather. The height and dynamics of the PBL (especially convection) can affect surface aerosol dynamics, especially with respect to particle concentrations. The PBL height was estimated using the lidar ceilometer with larger heights typically associated with stronger convective and thermal mixing. Seasonally averaged temperature and PBL heights agreed quite well (R^2 = 0.812) where seasons with higher temperatures had higher PBL heights, although there was not as strong of a correlation between daily averaged temperature and daily maximum PBL height (R^2 = 0.3) since deep boundary layers can still develop in the wintertime when temperatures are cold (see Figs. S1 and S2). During the summer and autumn, the PBL heights were at their highest (Table 1), so there was the most mixing and dilution of particles within the boundary layer. The summer and early autumn are associated with large amounts of solar radiation at the surface, leading to increased heating, which results in stronger thermals and convective mixing within the boundary layer. These processes both act to increase the boundary layer height, and tend to mix out and dilute the UFP concentration, which could also affect NPF initiation. On the other hand, during the wintertime, the boundary layers are at their lowest with weak thermals and mixing, so other particles were trapped near the surface, increasing the concentrations. Thus, due to lower temperatures and due to lower PBL heights, there were higher concentrations of UFP and higher NPF frequencies.

The average overall growth rate (during the entire growth period) of the median particle diameter during aerosol growth events in Huntsville was 1.7 ± 4.7 nm h^{-1} (Table 1) and had a range of 0.9–4.1 nm h^{-1} (Table S2). In comparison, observations showed growth rates in Ozark Forest in Missouri ranged from 1.6 to 11.2 nm h^{-1} (Yu et al., 2014), in Ohio rates from 0.5 to 12 nm h^{-1} (Kanawade et al., 2012), and in North Carolina from 1.6 to 5.7 nm h^{-1} (Meskhidze et al., 2019). Overall, the aerosol growth rates were slightly lower in Huntsville than at these locations (Table 1). The growth rates in the autumn were the largest (2.7 ± 3.9 nm h^{-1}), followed by winter (2.2 ± 4.8 nm h^{-1}), spring (1.8 ± 5.0 nm h^{-1}), then summer (1.2 ± 4.9 nm h^{-1}). Ambient temperature is also associated with NPF precursor emissions, e.g., with highest biogenic volatile organic compounds (VOCs) in the summer (Guenther et al., 2006). The fact that in summer, we still had lowest GR, emphasize the thermodynamics effects of lower temperatures on NPF. Compared to boreal forests in high latitudes with relatively lower temperatures year around, high emissions of monoterpenes in summer important for higher growth of new particles (Kerminen et al., 2018). But at our subtropical site, it is likely that the thermodynamics effects due to higher temperatures overweigh stronger biogenic emissions in summer.

Most often, particles larger than 100 nm are considered as a CCN proxy, but studies have shown that smaller particles (e.g., 60 nm or larger) can also act as CCN depending on chemical composition and atmospheric conditions (Kalivitis et al., 2015; Pöhlker et al., 2021). Of the growth events measured in Huntsville, only one of the 29 events (3%) resulted in a median particle diameter 100 nm or larger (Table S2); however, 15 of these growth events (52%) resulted in particles that grew to a median size of 60 nm or larger (Table S2). Across various locations globally, the percentage of NPF events that produce CCN-size particles range from approximately 10%–60%, within the range previously reported (Kerminen et al., 2018).

There are two main UFP sources at urban sites, primary particles emitted from traffic and secondary NPF processes (Brines et al., 2015; Hama et al., 2017; Hofman et al., 2016; Saha et al., 2018). From the measured size distributions, however, we found that UFP concentrations during the rush hours were usually significantly lower than during NPF. Thus, at our site, perhaps because it is located at the university campus, the UFP was mainly from NPF rather than traffic emissions. A recent study also indicated that at urban sites, traffic can also emit sub-3 nm particles (Rönkkö et al., 2017); another study also suggested that

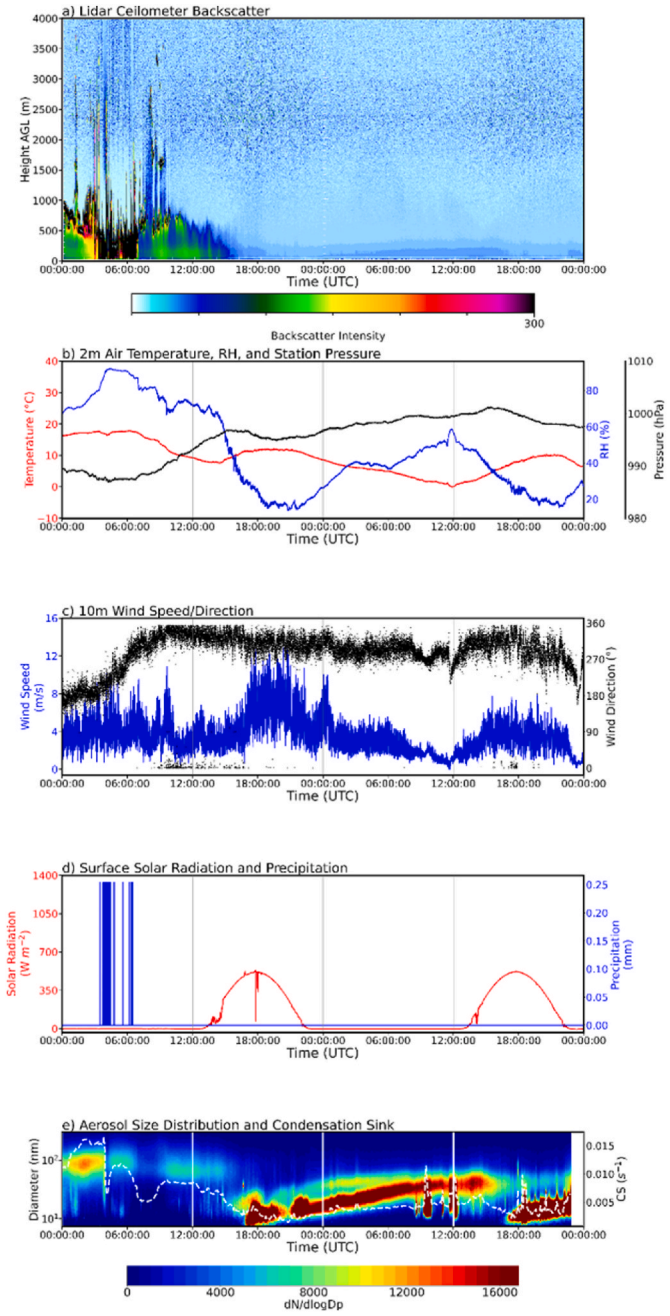

Fig. 2. Meteorological and aerosol measurements for 29–30 December 2016 including a) lidar ceilometer backscatter intensity, b) 2 m air temperature in °C (red line), 2 m RH in % (blue line), and station pressure in hPa (black line), c) 10 m wind speed in m•s^{-1} (blue line) and 10 m wind direction in degrees (black dots), d) solar radiation at the surface in W•m^{-2} and precipitation in mm, and e) 7–300 nm aerosol size distribution and condensation sink (CS) time series. All times are UTC. The local 06:00 and 18:00 are indicated as vertical bars.

oxygenated organics emitted from vehicle exhausts are largely responsible for urban NPF (Guo et al., 2020). In this context, we note that of the 29 NPF events in Tables S1 and 8 (28%) of them occurred near the rush hours.

3.2. Effects of meteorology on NPF initiation

One type of meteorological event thought to be of great importance to NPF initiation in Huntsville is a cold front passage. Out of the 29 NPF initiations reviewed in this study (Table S2), 22 of them occurred within 48 h of a cold front passage (76%, Table S3). Only five NPF events took place with a PBL height greater than 1000 m and 11 events took place with a PBL height of 500 m or less.

Fig. 2 shows the measured lidar ceilometer backscatter intensity, surface meteorological data, and aerosol size distributions on 29–30 December 2016 after a cold front passage at approximately 0600 UTC on 29 December. Extremely high lidar backscatter values (e.g., black color) are typically indicative of clouds and precipitation. Clouds can be seen from 0000 to 1000 UTC with precipitation from around 0300–0700 UTC on 29 December from Fig. 2a. This period of precipitation was also observed by the surface station, as seen in Fig. 2d. Shortly after the rainfall started, Fig. 2e shows the UFP concentrations immediately decreased to significantly lower values. The backscatter in the lidar was also lower after the rain than it was before the rain, indicating that larger particles were also scavenged from the PBL. These results indicate that precipitation scavenging may be an important process for creating a

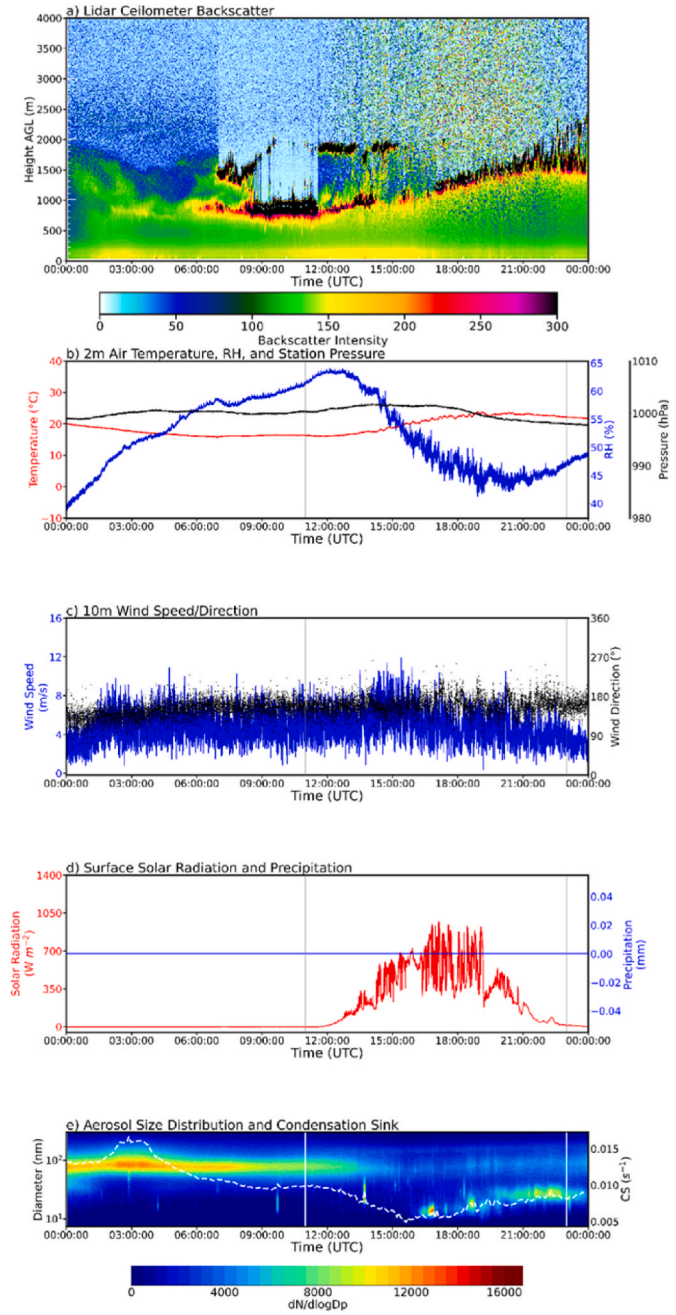

Fig. 3. Same as Fig. 2 but for 24 March 2017.

more favorable environment for NPF to occur.

The precipitation scavenging event discussed above was also associated with a cold front from a nearby low pressure system and associated advection of a modified maritime polar air mass, which acted to reduce the relative humidity, as seen in Fig. 2b. Since rainfall typically occurs with both frontal and cyclone passages, precipitation scavenging may be an important factor favoring for NPF ahead of the front. There are several factors that make post-cold frontal air masses favorable for NPF and aerosol growth. First, the air behind the front is generally clean. We observed that precipitation scavenging occurring ahead of the front. There were relatively high backscatter values near the surface while the clouds were present, indicating larger particles present in the PBL. Around 1500 UTC, the backscatter decreased significantly, indicating a lack of large particles in the PBL, likely due to the advection of cleaner air into the region, as well as the development of a convective PBL on the afternoon of 29 December. There was a sudden decrease in ultrafine particle concentrations around 0400 UTC, just after the precipitation began, and a NPF event initiated near 1700 UTC, 2 h after the backscatter decrease. At the time of NPF, the deep, dry, and vigorous mixing was occurring in the PBL, indicated by the low RH and gusty winds in Fig. 2b and c, respectively.

The growth event continued past 0000 UTC into December 30, as a result of prolonged periods of low backscatter and a clean PBL (Fig. 2). The initial growth event lasted until approximately 1500 UTC on 30 December. The concentrations of the resultant UFPs decreased, possibly due to dilution, and a new growth event initiated shortly after at around 1700 UTC. The conditions on 30 December appeared to be quite similar to the post-rain environment of the prior day with low RH and the development of a convective PBL.

Both NPF events occurred when RH was low, wind speeds were large and gusty (analog for high mixing), and near the daily peak of solar radiation, all shown in Fig. 2. All of these meteorological parameters (except for the wind speed) during the NPF initiation follow what is expected from previous findings (e.g. (Meskhidze et al., 2019)). The meteorological conditions were similar the next day, which supports why the aerosol dynamics behaved similarly. Cold fronts thus appear to provide a quite favorable environment for NPF to occur in Huntsville, Alabama. However, there were some cases where a cold front passage did not help to trigger a NPF initiation. A cold front passage occurred on 4 February, 2022, but there were no NPF initiations on 4–6 February, 2022 (Fig. S3). The reason for this is not immediately clear and should be investigated in the future.

Another trend in the boundary layer is that NPF is unfavorable if the PBL is dominated by large particles. In Fig. 2, the first NPF event did not initiate until after the lidar backscatter decreased, indicating the concentrations of relatively large particles had been reduced. Conversely, on 24 March 2017, the presence of large particles was detected by the ceilometer throughout the entire day (Fig. 3a). In addition to the high backscatter near the surface, there was also a cloud layer beginning at 0600 UTC that followed the top of the PBL, and low backscatter values were found above the PBL. The lidar also shows the diurnal evolution of the PBL, suggesting vigorous mixing was occurring. The spring season is a very common time for pollen production by vegetation, particularly oak and other trees, in the southeastern US (Saha et al., 2018). The high backscatter was likely caused by pollen being mixed in the PBL by the winds. The aerosol size distribution (Fig. 3e) shows moderate concentrations of CCN sized particles until about 0800 UTC, but the concentrations start decreasing after this time. After about 1400 UTC, there were few UFP present (Fig. 3e). A weak NPF and growth event tried to initiate around 1600 UTC, but the concentrations remained low throughout that entire event (Fig. 3e).

3.3. Sustained long-growth

Sustained particle growth events are defined as those that last for more than 12 h. In Table S2, all but five of the NPF initiations resulted in a growth event that was shorter than 12 h. The remaining 83% of NPF events resulted in these long growth events. These long growth events were the most common in the winter followed by the spring, similar to the NPF frequency. During both of these season, and the spring in particular, there were several back-to-back days of NPF and growth events taking place. The longest of these events was three days of repeated growth events on 8–10 February 2022 (Fig. 4). These long growth events were typically associated with the clean, cool air masses after a cold front passage as indicated by the reduction in lidar backscatter at 1700 UTC (Fig. 4a). The temperatures were unseasonably warm with clear skies and afternoon RH values near 25% (Fig. 4b) are all indicative of a convective boundary layer with vigorous mixing. The initiation of the NPF events near 1800 UTC (Fig. 4e) coincide with the reduction in lidar backscatter (Fig. 4a) and an increase in the wind speed and gusts (Fig. 4c), which both suggest vigorous mixing within the PBL, similar to the case in Fig. 2. The maximum frequency of cold fronts and

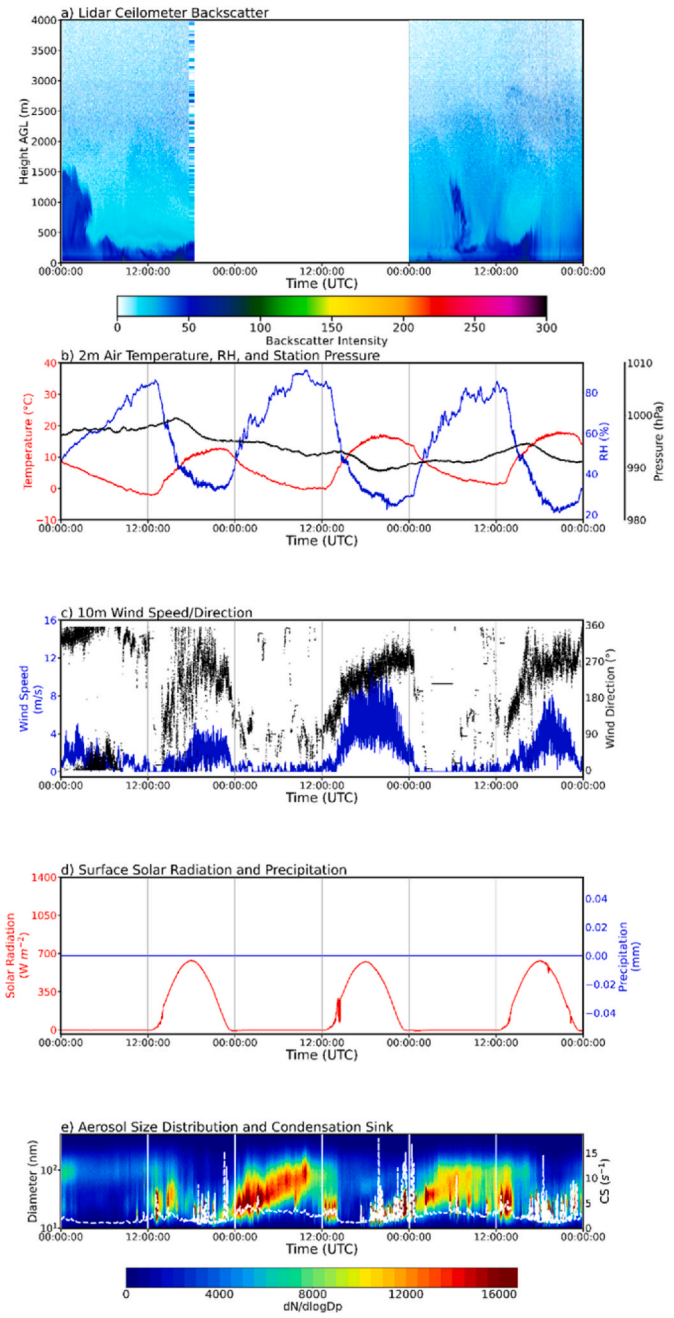

Fig. 4. Same as Fig. 2 but for 8–10 February 2022.

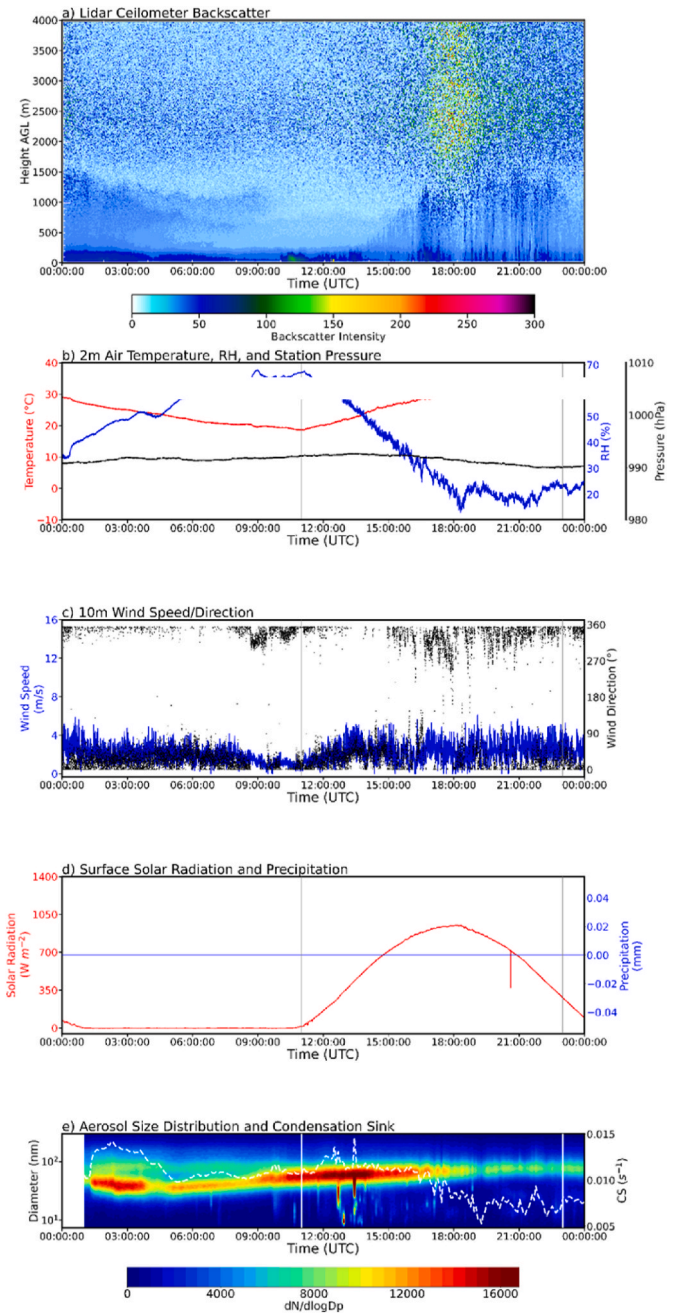

Fig. 5. Same as Fig. 2 but 30 June 2016.

the presence of cold air masses in the winter can help to explain the high amount of long aerosol growth events.

Even though the wintertime was seen to have lower PBL heights and higher UFP number concentrations, on average (Table 1), in this case, the PBL was more vigorous than normal for this time of year. Instead of seeing UFPs trapped near the surface, convective mixing acted to dilute them, a feature more common in summertime PBLs. Additionally, on 10 February 2022, there are rapid changes in the concentration of UFPs at the surface. Since there is not much dilution, this could be a case where non-local mixing and thermals dominate vertical transport within the PBL (Saha et al., 2018).

In the cases shown in Figs. 2 and 4, NPF and long growth events were associated with both deep PBLs and cool temperatures associated with synoptic scale weather disturbances. Fig. 5 shows lidar backscatter, surface measurements and aerosol size distribution for 30 June 2016. Similar to the other cases, Fig. 5a shows the PBL height was approximately 2000 m at 2100 UTC (although solar radiation contamination reduces the confidence in this estimate) and the RH decreased to near 25%, indicative of strong mixing (Fig. 5b). The aerosol size distribution in Fig. 5e also showed a growth event that initiated in the previous day that gradually ended (possibly due to dilution) at approximately 1700 UTC, similar to 30 December 2016 and 10 February 2022 in Fig. 2e and 4e; however, in this case, there was no initiation of NPF in the afternoon. The main difference is that the temperatures are much higher in Fig. 5b (about 30 °C) than in Fig. 2b or Fig. 4b (both are about 10 °C). This could be a result of high temperatures contributing to the thermodynamic instability of freshly nucleated UFPs.

4. Conclusions

From long-term measurements of 0–4 km lidar ceilometer backscatter profiles, surface meteorology parameters, and aerosol size distributions in the southeastern US, we identified cases where meteorology had a significant impact on the surface aerosol dynamics in Huntsville, Alabama. The most important meteorological event was cold front passages. There were consistent patterns of NPF followed by long aerosol growth events that were initiated several hours after the occurrence of precipitation scavenging and cooler, cleaner air moving into the region behind the front. Other meteorological events thought to have an impact are the boundary layer heights and convective mixing. NPF events occurred most frequently in the winter and least frequently in the summer, indicating that low temperatures are important for NPF in warm climates such as in the southeastern US.

Author contributions

ZW: made data analysis and wrote the manuscript, LT: made measurements, AP: provided comments on the manuscript, KK: made measurements, SHL: designed the research and wrote the manuscript.

Declaration of competing interest

The authors declare that they have no known competing financial interests or personal relationships that could have appeared to influence the work reported in this paper

Data availability

Data will be made available on request.

Acknowledgements

This research is supported by National Science Foundation (AGS-2209722). Zachary Watson was a participant of the NSF REU program at UAH (AGS-1757892).

Appendix A. Supplementary data

Supplementary data to this article can be found online at https://doi.org/10.1016/j.atmosenv.2023.119952.

References

Alabama Department of Transportation. Alabama Traffic Data. https://aldotgis.dot.state.al.us/TDMPublic/.

Boulon, J.K., et al., 2011. Investigation of nucleation events vertical extent: a long term study at two different altitude sites. Atmos. Chem. Phys. 11, 5625–5639.

Brines, M., et al., 2015. Traffic and nucleation events as main sources of ultrafine particles in high-insolation developed world cities. Atmos. Chem. Phys. 15 (10), 5929–5945.

Chen, H., et al., 2018. Vertically resolved concentration and liquid water content of atmospheric nanoparticles at the US DOE Southern Great Plains site. Atmos. Chem. Phys. 18, 311–326.

Fan, J.W., et al., 2018. Substantial convection and precipitation enhancements by ultrafine aerosol particles. Science 359 (6374), 411–418.
Guenther, A., et al., 2006. Estimates of global terrestrial isoprene emissions using MEGAN (model of emissions of gases and aerosols from nature). Atmos. Chem. Phys. 6, 3181–3210.
Guo, S., et al., 2020. Remarkable nucleation and growth of ultrafine particles from vehicular exhaust. Proc. Natl. Acad. Sci. USA 117 (7), 3427.
Hama, S.M.L., Cordell, R.L., Monks, P.S., 2017. Quantifying primary and secondary source contributions to ultrafine particles in the UK urban background. Atmos. Environ. 166, 62–78.
Hofman, J., et al., 2016. Ultrafine particles in four European urban environments: results from a new continuous long-term monitoring network. Atmos. Environ. 136, 68–81.
Kalivitis, N., et al., 2015. Atmospheric new particle formation as a source of CCN in the eastern Mediterranean marine boundary layer. Atmos. Chem. Phys. 15, 9203–9215.
Kanawade, V., Benson, D.R., Lee, S.H., 2012. Statistical analysis of 4 year measurements of aerosol sizes in a semi-rural U.S. continental environment. Atmos. Environ. 59, 30–38.
Kerminen, V.M., et al., 2018. Atmospheric new particle formation and growth: review of field observations. Environ. Res. Lett. 13 (10), 38.
Kulmala, M., et al., 1998. Analysis of the growth of nucleation mode particles observed in Boreal forest. Tellus 50, 449–462.
Lai, S., et al., 2022. The striking effect of vertical mixing in the planetary boundary layer on new particle formation in the Yangtze River Delta. Sci. Total Environ. 829, 154607.
Lampilahti, J., et al., 2021. Aerosol particle formation in the upper residual layer. Atmos. Chem. Phys. 21 (10), 7901–7915.
Lee, S.-H., et al., 2019. New Particle Formation in the atmosphere: from molecular clusters to global climate. J. Geophys. Res. Atmos. 124 (13), 7098–7146.
Liu, Y., et al., 2021. Impact of residual layer transport on air pollution in Beijing, China. Environ. Pollut. 271, 116325.
Meskhidze, N., et al., 2019. Possible wintertime sources of fine particles in an urban environment. J. Geophys. Res. Atmos. 124 (23), 13055–13070.
Nilsson, E.D., et al., 2001. Effects of continental boundary layer evolution, convection, turbulence and entrainment, on aerosol formation. Tellus B 53 (4), 441–461.
Nyeki, S., et al., 1999. Condensation nuclei (CN) and ultrafine CN in the free troposphere to 12km: a case study over the Jungfraujoch high-alpine research station. Geophys. Res. Lett. 26, 2195–2198.
Pöhlker, M.L., et al., 2021. Aitken mode particles as CCN in aerosol- and updraft-sensitive regimes of cloud droplet formation. Atmos. Chem. Phys. 21 (15), 11723–11740.
Rönkkö, T., et al., 2017. Traffic is a major source of atmospheric nanocluster aerosol. Proc. Natl. Acad. Sci. USA 114 (29), 7549.
Saha, P.K., et al., 2018. Reduced ultrafine particle concentration in urban air: changes in nucleation and anthropogenic emissions. Environ. Sci. Technol. 52 (12), 6798–6806.
Siebert, H., Stratmann, F., Wehner, B., 2004. First observations of increased ultrafine particle number concentrations near the inversion of a continental planetary boundary layer and its relation to ground-based measurements. Geophys. Res. Lett. 31 (9).
Stull, R.B., 1998. In: Plate, E.J., Fedorovich, E.E., Viegas, D.X., Wyngaard, J.C. (Eds.), Transilient turbulence theory: a nonlocal description of convection, Buoyant Convection in Geophysical Flows. NATO ASI Series, vol. 513. Springer, Dordrecht.
Wang, J., et al., 2016. Amazon boundary layer aerosol concentration sustained by vertical transport during rainfall. Nature 539 (7629), 416–419.
Wang, Y., et al., 2023. Sulfur dioxide transported from the residual layer drives atmospheric nucleation during haze periods in Beijing. Geophys. Res. Lett. 50 (6), e2022GL100514.
Wehner, B., et al., 2010. Observations of turbulence-induced new particle formation in the residual layer. Atmos. Chem. Phys. 10, 4319–4330.
Williamson, C.J., et al., 2019. A large source of cloud condensation nuclei from new particle formation in the tropics. Nature 574 (7778), 399–403.
Wu, H., et al., 2021. The impact of the atmospheric turbulence-development tendency on new particle formation: a common finding on three continents. Natl. Sci. Rev. 8 (3).
Yu, H., Ortega, J., Smith, J.N., Guenther, A.B., Kanawade, V.P., You, Y., Liu, Y., Hosman, K., Karl, T., Seco, R., Geron, C., Pallardy, S.G., Gu, L., Mikkilä, J., Lee, S.-H., 2014. New Particle Formation and growth in an isoprene-dominated Ozark forest: from sub-5 nm to CCN-active sizes. Aerosol. Sci. Technol. 48 (12), 1285–1298.
Zhang, S., Lyu, Y., Yang, X., Yuan, L., Wang, Y., Wang, L., Liang, Y., Qiao, Y., Wang, S., 2022. Modeling biogenic volatile organic compoints emissions and subsequent impacts on ozone air quality in the sichuan basin, southwestern China. Front. Ecol. Evol. 10.